

# Simulation of QED Radiation in Particle decays using the YFS Formalism

---

**Keith Hamilton and Peter Richardson**

*Institute of Particle Physics Phenomenology, Department of Physics*

*University of Durham, Durham, DH1 3LE, UK*

*Email: keith.hamilton@durham.ac.uk, peter.richardson@durham.ac.uk*

**ABSTRACT:** In this paper we describe a program (SOPHTY) implementing QED corrections to decays in the HERWIG++ event generator. In order to resum the dominant soft emissions to all orders, the program is based on the YFS formalism. In addition, universal large collinear logarithms are included and the approach can be systematically extended to incorporate exact, process specific, higher order corrections to decays. Due to the large number of possible decay modes the program is designed to operate, as far as possible, independently of the details of the decay matrix elements.

**KEYWORDS:** LEP HERA and SLC Physics, Electromagnetic Processes and Properties, Weak Decays.

---

## Contents

<b>1. Introduction</b>	<b>1</b>
<b>2. Algorithms</b>	<b>4</b>
2.1 Final-Final Dipole	7
2.2 Initial-Final Dipole	11
<b>3. Higher-Order Corrections</b>	<b>13</b>
3.1 Real Emission Corrections: $\bar{\beta}_1^1$	14
3.2 Virtual Corrections: $\bar{\beta}_0^1$	16
<b>4. Results</b>	<b>17</b>
<b>5. Conclusions</b>	<b>21</b>
<b>A. YFS Form Factors</b>	<b>24</b>
A.1 Final-Final Dipoles	24
A.2 Initial-Final Dipoles	25
<b>B. Generation of the Dipole Distributions</b>	<b>25</b>
B.1 Final-Final Dipoles	26
B.2 Initial-Final Dipoles	27

---

## 1. Introduction

The use of Monte Carlo event generators has become an essential part of all experimental analyses, both in interpreting data from existing experiments and in the design and planning of future experiments. Given the crucial rôle which Monte Carlo simulations play in experimental studies it is imperative that these simulations are as accurate as possible.

While the existing Monte Carlo event generators have been highly successfully over the last twenty years, it was realised that a new generation of programs was necessary for the LHC. The reasons for this were twofold: firstly a number of new ideas to improve the accuracy of the simulations had been suggested *e.g.* [1–4]; secondly the existing programs required major restructuring for long term maintenance

and to allow new theoretical developments to be incorporated. Given the changing nature of computing in high energy physics, the natural choice was to write these new programs in C++. A major effort is therefore underway, in preparation for the LHC, to produce completely new event generators [5], as well as new versions of established simulations [6–10] in C++.

As part of the process of writing the new HERWIG++ event generator [8–10] we wish to improve many aspects of the simulation process. One area where improvements were needed was in the simulation of particle decays, both of the fundamental particles produced in the perturbative stages of the event and the decays of unstable hadrons. Several major improvements have been made to the simulation of the decays: better modelling of the matrix elements in hadronic decays; and full spin correlations between the production and decay of particles [11]. Another problem with the particle decays in the FORTRAN version of the HERWIG program was the absence of QED radiation, which we will address in this paper.

In existing Monte Carlo simulations the production of QED radiation in particle decays is normally simulated using an interface to the PHOTOS program [12–14]. This program is based on the collinear approximation for the radiation of photons together with corrections to reproduce the correct result in the soft limit [12, 13]. Recently, it has been improved to include the full next-to-leading order QED corrections for certain decay processes [14].

Despite the success of PHOTOS it is based on the collinear approximation for photon radiation. The production of radiation in these decays is normally simulated in the rest frame of the decaying particle. The kinematics of many of the decays, particularly of the unstable hadrons, is such that the energy of the decay products is not significantly larger than their mass, in which case we do not expect the collinear limit to be a good approximation. However, there is always a soft enhancement for the emission of QED radiation. We therefore chose to base the simulation of QED radiation in HERWIG++ on the YFS [15] formalism for the resummation of soft logarithms. This formalism has the major advantage that the exact higher-order corrections can be systematically included, indeed the majority of the most accurate simulations including higher-order QED corrections are based on this approach [16–23].

Another significant improvement arises from the use of the C++ programming language and an object-oriented design for the program. The code framework governing decays, in the HERWIG++ program, is arranged so that users can easily introduce the matrix element for a particular decay mode using the C++ inheritance mechanism. This framework also allows the inclusion of additional next-to-leading order matrix elements for both standard HERWIG++ and user defined decays. This makes it possible for the leading-order matrix elements and their higher-order corrections to be implemented in a systematic and consistent manor, rather than relying on one program to handle the leading-order decay and another for the higher-order

corrections. This will be of particular importance for the implementation of spin correlation effects. Moreover, it will be easier for users to introduce new decays, including higher-order corrections, as they will only require knowledge of, and make modifications to, one program rather than two.

Note that, in full generality, it is not possible to consider radiative corrections to production and decay processes separately<sup>1</sup>, the minimal requirement for such a treatment to preserve gauge invariance is that the intermediate particle be on-shell. For most applications at hadron colliders we anticipate this to be a good approximation. At a technical level this amounts to neglecting off-shell effects in propagator numerators and including finite width effects in propagator denominators via an overall Breit-Wigner factor that multiplies the squared amplitude (the so-called *narrow width approximation*). This approximation is already in effect at the level of the tree amplitudes in the HERWIG++ generator, in which spin correlation effects are transmitted from the production stage to the decay stage according to the algorithm described in [1]. As the SOPHTY program is to dress tree-level events generated by the HERWIG++ simulation, a more subtle treatment including off-shell effects is beyond the scope of this work.

The same approximation scheme is adopted in many other generators *e.g.* the PHOTOS and WINHAC [21] generators. Working in this approximation means that gauge invariance of the QED corrections is then guaranteed by considering only the universal leading log corrections to individually decays in a cascade. *Exact*  $\mathcal{O}(\alpha)$  corrections, comprising of additional *non-factorizable corrections* are process-specific, and are therefore the subject of dedicated process-specific simulations; the SOPHTY paradigm is primarily one of universality and general applicability. Nevertheless, the dominant corrections are due to universal soft and collinear enhanced terms.

In the next section we will present our master equation, based on the YFS formalism, for the generation of QED radiation, for the specific case of particle decays. High multiplicity *i.e.* greater than two body, particle decays are normally simulated as a series of sequential two body decays in HERWIG++. We therefore concentrate on the cases of the decay of a neutral particle to two charged particles and the decay of a charged particle to one charged and one neutral particle. In addition, we present algorithms for the event generation, using the master equation, for these two cases. The inclusion of higher-order corrections to the decays is then considered in section 3 followed by a discussion of the results of the simulation. Finally we present our conclusions and plans for further developments.

---

<sup>1</sup>The case of W boson production is a noteworthy example since it is both charged and unstable. This case has been studied in detail in the context of the charged Drell-Yan process [24–30] as well as single W production at LEP [31, 32].

## 2. Algorithms

We begin by considering the  $n$ -body decay of a particle in the *absence* of photonic radiation. The partial width for such a decay is given by

$$\int d\Gamma_0 = \frac{1}{2M} \int d\Phi_q (2\pi)^4 \delta^4 \left( p - \sum_{i=1}^n q_i \right) \rho_{\alpha\beta} \mathcal{M}_\alpha \mathcal{M}_\beta^* \quad (2.1)$$

where

$$d\Phi_q = \prod_{i=1}^n \frac{d^3 q_i}{(2\pi)^3 2q_i^0}, \quad (2.2)$$

$M$  is the mass of the decaying particle,  $p$  is its four-momentum and  $q_i$  is the momenta of the  $i$ th decay product. We have also denoted the matrix element for the decay of a particle with helicity  $\alpha$  by  $\mathcal{M}_\alpha$  and  $\rho_{\alpha\beta}$  represents the spin density matrix. In order to simplify the expressions we have suppressed the dependence of the matrix element on the momenta of the decaying particle and the decay products. In practice we do not need to include the spin density matrix when calculating the total width, if we wish to average over the helicities of the decaying particles it is simply the identity matrix. However, inside the HERWIG++ simulation it allows us to include the correlation effects for the decay.

In order to simulate the effects of additional QED radiation in the decay, we must generalise (2.1) to include the effects of arbitrary numbers of photons. In principle this extension is straightforward; one simply replaces the matrix element and augments the phase space. However, the matrix elements give rise to infrared divergences. The cancellation of these soft divergences must be made explicit before the Monte Carlo integration over the phase space can be performed.

In the YFS formalism this cancellation of the divergences is manifest to all orders in perturbation theory. The cancellation relies on the fact that in the divergent, soft photon, limit both real and virtual corrections, to *any* process, take the form of universal kinematic factors multiplying the amplitude for that process without the additional radiation. In summing over all of the different soft photon contributions, these kinematic factors separately exponentiate, due to their universal nature. The resulting product of exponentials is the manifestly finite YFS form factor [15]. Residual, non-factorizing, parts of the matrix elements, which cannot be exponentiated, are naturally infrared finite.

Applying the YFS formalism to particle decays, by analogy to [17, 18, 33], we find that radiation modifies the  $n$ -body decay rate (2.1) to

$$\Gamma = \frac{1}{2M} \sum_{n_\gamma=0}^{\infty} \int d\Phi \frac{1}{n_\gamma!} e^{Y_{\text{total}}(\Omega)} \prod_{i=1}^{n_\gamma} \tilde{S}_{\text{total}}(k_i) \rho_{\alpha\beta} \mathcal{M}_\alpha \mathcal{M}_\beta^* \mathcal{C}. \quad (2.3)$$

This is the master equation from which we intend to generate the QED radiation, where

$$d\Phi = d\Phi_p d\Phi_k (2\pi)^4 \delta^4(p - P - K), \quad (2.4)$$

$K = \sum_{i=1}^{n_\gamma} k_i$  denotes the sum of photon momenta and  $P = \sum_{i=1}^n p_i$  denotes the sum of the primary decay products momenta. The momentum of the  $i$ th decay product is  $p_i$  (previously  $q_i$  without the photon radiation),  $k_j$  is the momentum of the  $j$ th photon, while  $d\Phi_p$  and  $d\Phi_k$  are the associated phase space measures:

$$d\Phi_p = \prod_{i=1}^n \frac{d^3 p_i}{(2\pi)^3 2p_i^0}; \quad (2.5)$$

$$d\Phi_k = \prod_{i=1}^{n_\gamma} \frac{d^3 k_i}{k_i^0} \Theta(k_i, \Omega).$$

The symbol  $\Omega$  is used to denote the region of phase space *inside* which photons are soft and unresolvable, we choose this to be the region  $|\vec{k}| < \omega$ , with  $\omega$  an energy cut-off. We define  $\Theta(k_i, \Omega) = 0$  for  $k_i \in \Omega$  and  $\Theta(k_i, \Omega) = 1$  for  $k_i \notin \Omega$ . This definition of  $\Omega$  is not Lorentz invariant and in addition to specifying a value for  $\omega$  we must specify the frame in which it has this value.

The total dipole radiation function

$$\tilde{S}_{\text{total}}(k) = \sum_{i < j}^n \tilde{S}(p_i, p_j, k) \quad (2.6)$$

is the sum of the individual dipole functions

$$\tilde{S}(p_i, p_j, k) = \frac{\alpha}{4\pi^2} Z_i \theta_i Z_j \theta_j \left( \frac{p_i}{p_i \cdot k} - \frac{p_j}{p_j \cdot k} \right)^2, \quad (2.7)$$

where  $k$  is the four momentum of the photon,  $Z_i$  is the charge of the  $i$ th particle in units of the positron charge and  $\theta_i = +1 (-1)$  if the momentum  $p_i$  is outgoing (incoming).

Likewise, the YFS form factor [15],  $Y_{\text{total}}(p_i, p_j, \Omega)$ , is given in terms of the form factor for pairs of charged particles

$$Y_{\text{total}}(p_i, p_j, \Omega) = \sum_{i < j}^n Y(p_i, p_j, \Omega). \quad (2.8)$$

The YFS form factor for a pair of charged particles is given by

$$Y(p_i, p_j, \Omega) = 2\alpha \left( \mathcal{R}e B(p_i, p_j, \Omega) + \tilde{B}(p_i, p_j) \right), \quad (2.9)$$

where  $\tilde{B}_{ij}$  is the integral of the dipole radiation function over the soft photon phase space

$$\tilde{B}(p_i, p_j, \Omega) = \frac{1}{8\pi^2} Z_i \theta_i Z_j \theta_j \int_{\Omega} \frac{d^3 k}{|\vec{k}|} \left( \frac{p_i}{k \cdot p_i} - \frac{p_j}{k \cdot p_j} \right)^2. \quad (2.10)$$

The virtual piece of the dipole

$$B(p_i, p_j) = -\frac{i}{8\pi^3} Z_i \theta_i Z_j \theta_j \int d^4k \frac{1}{k^2} \left( \frac{2p_i \theta_i - k}{k^2 - 2k \cdot p_i \theta_i} + \frac{2p_j \theta_j + k}{k^2 + 2k \cdot p_j \theta_j} \right)^2, \quad (2.11)$$

does not depend on the cut-off, it is plainly Lorentz invariant.

The form factors are given for the case of a neutral particle decaying to two charged final-state particles in Appendix A.1 and a charged particle decaying to one charged and one neutral particle in Appendix A.2, in the rest frame of the decay products. For the case of a general moving frame only modifications to the Lorentz variant bremsstrahlung integrals are needed, in the final step where we have simplified with  $\vec{p}_i = -\vec{p}_j$  and  $E_i + E_j = M$ . The corresponding  $\tilde{B}_{ij}$  functions are given in a general frame in [34] and [21] respectively.

The factor  $\mathcal{C}$  represents the total remainder of all of the matrix elements contributing to the total decay width for the particle, including any number of photons, when the leading soft divergent pieces are exponentiated and cancelled. The contents of  $\mathcal{C}$  are referred to as the *infrared residuals*, they are infrared finite and are written as a power expansion in the electromagnetic coupling  $\alpha$ .

To order  $\alpha$  there are three infrared residuals: the leading-order matrix element ( $\mathcal{O}(\alpha^0)$ ), the finite remainder of the one loop correction to the leading-order process and the finite residual of the single photon emission matrix element. Using superscripts to denote the order in  $\alpha$  and subscripts to denote the number of emitted photons, we have

$$\mathcal{C} = 1 + \frac{1}{\rho_{\alpha\alpha'} \mathcal{M}_\alpha \mathcal{M}_{\alpha'}^*} \left( \bar{\beta}_0^1(p, \{p_i\}) + \sum_{j=1}^{n_\gamma} \frac{\bar{\beta}_1^1(p, \{p_i\}, k_j)}{\tilde{S}_{\text{total}}(k_j)} + \mathcal{O}(\alpha^2) \right), \quad (2.12)$$

where

$$\begin{aligned} \bar{\beta}_0^1(p, \{p_i\}) &= \rho_{\alpha\beta} (\mathcal{M}_\alpha \mathcal{M}_{V\beta}^{1*} + \mathcal{M}_{V\alpha}^1 \mathcal{M}_\beta^* - 2\alpha B_{\text{total}} \mathcal{M}_\alpha \mathcal{M}_\beta^*) \\ \bar{\beta}_1^1(p, \{p_i\}, k) &= \rho_{\alpha\beta} \left( \frac{1}{2(2\pi)^3} \mathcal{M}_{R\alpha}^1 \mathcal{M}_{R\beta}^{*1} - \tilde{S}_{\text{total}}(k) \mathcal{M}_\alpha \mathcal{M}_\beta^* \right). \end{aligned} \quad (2.13)$$

In (2.13) we use  $\mathcal{M}_R^1$  and  $\mathcal{M}_V^1$  to denote the  $\mathcal{O}(\alpha)$  corrections to the leading-order matrix element ( $\mathcal{M}$ ) from single real and single virtual photon corrections. The extension of the master formula to higher orders in the infrared residuals ( $\bar{\beta}$ ) is straightforward, it is only limited by the usual technical difficulties associated with calculating Feynman diagrams that involve many loops or legs.

In practice the leading-order matrix element is only strictly defined for the  $n$ -body phase space, not the phase space with additional photons. We therefore need a procedure which maps the momenta of the decay products after radiation, including the photons, on to the momentum configuration of the decay products prior to the generation of any radiation. Since the momenta of the primary decay products

are to be generated first before any QED radiation, according to the leading-order distribution, we can use these momenta to calculate the leading-order matrix element.

In order to implement the theoretical framework of the master equation in an event generator, one expects that a number of different algorithms must be devised to cope with all possible decay multiplicities and charge configurations. In practice, due to the way in which particle decays are simulated in HERWIG++, most of the decays will either involve the decay of a charged particle to one charged and one neutral particle, or the decay of a neutral particle to two charged particles. Furthermore, we anticipate that more complicated decays will proceed via repeated applications and simple extensions of these two types of decay. We therefore concentrate on these cases.

## 2.1 Final-Final Dipole

The purpose of this algorithm is to *dress* the decays, generated by the core HERWIG++ program, in which a neutral particle decays to two charged particles, with QED radiation. The input to our algorithm therefore consists of the momenta and quantum numbers of the parent particle and its children, distributed according to the leading-order differential decay rate (2.1).

In addition to infrared singularities, the dipole functions (2.7) also exhibit mass singular behaviour associated with small-angle photon emission from the charged particles, in the massless limit. Therefore the angles of the radiated photons with respect to the dipole must remain fixed throughout the event generation process in order to produce an efficient, stable algorithm.

In order to achieve this, we define the rest frame of the primary decay products and generate the photons in this frame. In this respect our approach is similar to that used in the  $\mathcal{K}\mathcal{K}$  event generator [20] for final-state radiation. Initially the photons are generated according to the dipole functions, which have a simple form in this frame. Implicit in the definition of the rest frame of the primary decay products (in this case the dipole) is the fact that the *incoming* three-momentum of the decaying particle must be equal to the *total outgoing* three-momentum of the photons. The three-momenta of the original decay products are then rescaled (reduced) to ensure energy and momentum conservation.

A naïve application of the method outlined above will lead to spurious results. It is important that we take into account the effects of the aforesaid choice of frame on the phase-space integration measure. To do this we employ the method of integration over the Lorentz group, as described in [35], to transform the phase-space measure in (2.3). We start, by introducing the definition of the momentum of the decaying particle and the total momentum of the primary decay products in terms



of  $\delta$ -functions, assuming the full phase space is to be integrated over *i.e.*

$$\int d\Phi = (2\pi)^4 \int d\Phi_p d\Phi_k d^4p ds d^4P 2M\delta^3(p) \delta(p^2 - M^2) \quad (2.14)$$

$$\delta^4(p - P - K) \delta^4\left(P - \sum_{i=1}^n p_i\right) \delta(P^2 - s).$$

Secondly we insert the identity

$$\int d^4X \frac{2}{s^2} \delta\left(\frac{X^2}{s} - 1\right) \delta^3\left(L^{-1} \frac{P}{\sqrt{s}}\right) = 1, \quad (2.15)$$

where  $L^{-1}$  is the boost *from* the frame in which  $X = (X_0, \vec{X})$  *to* the rest frame of  $X$ . This identity, in conjunction with those already present in (2.14), constrains the boost  $L$  to be the Lorentz transformation from the rest frame of the primary decay products ( $P$ ) to the rest frame of the decaying particle ( $p$ ). We then change the integration variables, by applying the Lorentz boost  $L$  to all of the momenta involved, which is trivial as most of our expression (2.14) is Lorentz invariant. This gives

$$\int d\Phi = (2\pi)^4 \int d\Phi_p d\Phi_k d^4p ds d^4P d^4X \delta^3(Lp) \delta(p^2 - M^2) \quad (2.16)$$

$$\delta^4(p - P - K) \delta^4\left(P - \sum_{i=1}^n p_i\right) \delta(P^2 - s) \frac{4M}{s^2} \delta\left(\frac{X^2}{s} - 1\right) \delta^3\left(\frac{P}{\sqrt{s}}\right).$$

Integrating over the four momentum  $P$ ,  $X$  and  $p$  we obtain

$$\int d\Phi = (2\pi)^4 \int d\Phi_p d\Phi_k ds \frac{s}{M^2} \delta(M^2 - (P + K)^2) \delta^4\left(P - \sum_{i=1}^n p_i\right). \quad (2.17)$$

The integral over  $s$  can then be performed giving,

$$\int d\Phi = \int d\Phi_p d\Phi_k \frac{s}{M^2 \left(1 + \frac{K_0}{\sqrt{s}}\right)} (2\pi)^4 \delta^4\left(P - \sum_{i=1}^n p_i\right). \quad (2.18)$$

As we first generate the momenta of the other decay products according to the leading-order matrix element we need to rewrite the integral in terms of the leading-order phase space. This is achieved by rescaling the momenta of the decay products before radiation to give the correct invariant mass for the decay products after the photon radiation. We define a momentum rescaling factor,  $u$ , such that the three momenta obey  $\vec{q}_i = u\vec{p}_i$ . The momentum rescaling  $u$  is determined, by on-shell constraints, to be the solution of

$$\sum_i^n \sqrt{u^2 |\vec{q}_i|^2 + m_i^2} - \sqrt{s} = 0, \quad (2.19)$$

where  $m_i^2 = p_i^2 = q_i^2$ .

The unitary algorithm techniques of [36] can be used to show that

$$\int d\Phi_p \delta^4 \left( P - \sum_{i=1}^n p_i \right) = \int d\Phi_q \delta^4 \left( Q - \sum_{i=1}^n q_i \right) \frac{1}{u^3} \frac{\left( M - \sum_{i=1}^n \frac{m_i^2}{q_i^0} \right)}{\left( \sqrt{s} - \sum_{i=1}^n \frac{m_i^2}{p_i^0} \right)} \prod_{i=1}^n \frac{q_i^0 u^3}{p_i^0}. \quad (2.20)$$

With this result we can rewrite our phase space measure as

$$\int d\Phi = \int d\Phi_q d\Phi_k (2\pi)^4 \delta^4 \left( Q - \sum_{i=1}^n q_i \right) \frac{s^{\frac{3}{2}}}{M^2 (\sqrt{s} + K_0)} \frac{1}{u^3} \frac{\left( M - \sum_{i=1}^n \frac{m_i^2}{q_i^0} \right)}{\left( \sqrt{s} - \sum_{i=1}^n \frac{m_i^2}{p_i^0} \right)} \prod_{i=1}^n \frac{q_i^0 u^3}{p_i^0}. \quad (2.21)$$

The decay width becomes

$$\Gamma = \sum_{n_\gamma=0}^{\infty} \frac{1}{n_\gamma!} \int d\Gamma_0 d\Phi_k e^{Y_{\text{total}}(\Omega)} \prod_{i=1}^{n_\gamma} \tilde{S}_{\text{total}}(k_i) \mathcal{C} \frac{s^{\frac{3}{2}}}{M^2 u^3 (\sqrt{s} + K_0)} \frac{\left( M - \sum_{i=1}^n \frac{m_i^2}{q_i^0} \right)}{\left( \sqrt{s} - \sum_{i=1}^n \frac{m_i^2}{p_i^0} \right)} \prod_{i=1}^n \frac{q_i^0 u^3}{p_i^0} \quad (2.22)$$

with  $d\Gamma_0$  given by (2.1). Equation (2.22) allows the construction of an algorithm in which the leading-order subprocess may be generated independently of and prior to QED radiation.

Thus far we have treated the general case (an  $n$  body final state) but we will now specialise to the case of a neutral particle decaying to two charged particles. In this case the rescaling factor is  $u = |\vec{p}|/|\vec{q}|$  where  $|\vec{p}|$  is the magnitude of the momentum of the decay products in their rest frame after the radiation and  $|\vec{q}|$  is the magnitude of the momentum of the decay products in their rest frame before the radiation. In this case the total width is

$$\Gamma = \sum_{n_\gamma=0}^{\infty} \int d\Gamma_0 d\Phi_k \frac{1}{n_\gamma!} e^{Y_{\text{total}}(\Omega)} \prod_{i=1}^{n_\gamma} \tilde{S}_{\text{total}}(k_i) \mathcal{C} \frac{\sqrt{s} |\vec{p}|}{M |\vec{q}|} \left( 1 + \frac{K_0}{\sqrt{s}} \right)^{-1}, \quad (2.23)$$

where

$$d\Gamma_0 = \frac{1}{2M} d\Omega_{q_2} \frac{|\vec{q}|}{M} \rho_{\alpha\beta} \mathcal{M}_\alpha \mathcal{M}_\beta^*.$$

Up to now we have not made *any* approximations other than the truncation of the infrared residuals at  $\mathcal{O}(\alpha)$ . To simulate events using these results, (2.23) and (2.22), we need to make some approximations in order to obtain a distribution which is fast and efficient to generate by Monte Carlo methods. It is important to note that these simplifications are later *exactly* compensated by appropriate weighting and rejection of events. Naturally the first simplification we make is to omit the higher-order, infrared finite corrections represented by the factor  $\mathcal{C}$ . We also neglect the factors associated with the rescaling of the leading-order phase space. Both factors tend to one in the limit of soft QED radiation and so neglecting them is reasonable,

given that the vast majority of photons produced will be soft. In addition to these two omissions we also approximate the momenta  $p_1$  and  $p_2$  by the values they would have in the absence of any QED radiation,  $q_1$  and  $q_2$ , this approximation is justified on the same grounds. These simplifications give the following *crude* distribution

$$\Gamma_{\text{crude}} = \sum_{n_\gamma=0}^{\infty} \int d\Gamma_0 d\Phi_k \frac{1}{n_\gamma!} e^{Y(q_1, q_2, \Omega)} \prod_{i=1}^{n_\gamma} \tilde{S}(q_1, q_2, k_i). \quad (2.24)$$

Since we are working in the dipole rest frame,  $\vec{q}_1 = -\vec{q}_2$ , the kinematics simplify to the extent that the dipole function is analytically integrable. Moreover it means the only dependence of the QED part of (2.24) on  $q_1$  and  $q_2$  is through their masses. Consequently we have the desired factorization that (2.24) is really a product of two separate integrals, one for the leading-order decay and one for the QED radiation. The distributions may therefore be generated independently. Defining

$$\bar{n} = \int \frac{d^3 k_i}{k_i^0} \Theta(k_i, \Omega) \tilde{S}(p_1, p_2, k_i), \quad (2.25)$$

we obtain

$$\Gamma_{\text{crude}} = \Gamma_0 \sum_{n_\gamma=0}^{\infty} \frac{1}{n_\gamma!} \bar{n}^{n_\gamma} e^{-\bar{n}} = \Gamma_0. \quad (2.26)$$

In deriving (2.26) we have also made the approximation that the YFS form factor is  $Y \approx -\bar{n}$ . According to  $\Gamma_{\text{crude}}$  the photon multiplicity follows a Poisson distribution with average  $\bar{n}$ . In practice it is sometimes useful to neglect part of the dipole distribution as described in Appendix B.1.

Once such a decay has been generated in the main HERWIG++ code it may be dressed with QED radiation using the following algorithm:

1. The number of photons is generated according to a Poisson distribution with average  $\bar{n}$ .
2. The momenta of the photons is then generated as described in Appendix B.1. This gives the crude distribution.
3. The exact distribution (the master equation for  $\Gamma$ ) is obtained using rejection techniques. The weight for rejection is given by

$$\mathcal{W} = \mathcal{W}_{\text{dipole}} \times \mathcal{W}_{\text{YFS}} \times \mathcal{W}_{\text{Jacobian}} \times \mathcal{W}_{\text{higher}}, \quad (2.27)$$

where

$$\begin{aligned} \mathcal{W}_{\text{dipole}} &= \prod_{i=1}^{n_\gamma} \frac{\tilde{S}(p_1, p_2, k_i)}{\tilde{S}(q_1, q_2, k_i)}, \\ \mathcal{W}_{\text{YFS}} &= \frac{e^{Y(p_1, p_2, \Omega_B)}}{e^{-\bar{n}}}, \\ \mathcal{W}_{\text{Jacobian}} &= \frac{\sqrt{s} |\vec{p}|}{M |\vec{q}|} (\sqrt{s} + K_0)^{-1}, \\ \mathcal{W}_{\text{higher}} &= \mathcal{C}. \end{aligned} \quad (2.28)$$

In practice the denominator of the dipole weight  $\mathcal{W}_{\text{dipole}}$  is modified if we use the modified dipole without the mass terms. We denote a cut-off on the energy of the photons in the rest frame of the decay products as  $\Omega_B$ . We will consider the contribution from the exact higher-order corrections in more detail in the next section.

4. There is one remaining complication. The photons are generated in the frame where the decaying particle enters with momentum equal to the total photon momentum. However, we wish to apply the energy cut-off in either the rest frame of the decaying particles, or even the laboratory frame. There are a number of methods which we could use to achieve this. The simplest would be to evaluate the YFS form-factor in the rest frame of the decaying particle or the laboratory frame and veto any events in which any of the photons are below the cut-off in the relevant frame. However, this procedure can be inefficient if the veto removes a large number of events.

We instead choose to use the same procedure as [20]. In this approach we neglect any photons which are below the energy cut-off in the relevant frame and apply an additional weight

$$\mathcal{W}_{\text{remove}} = \exp(-Y_{12}(q_1, q_2, \Omega_B) + Y_{12}(q_1, q_2, \Omega) + Y_{12}(p_1, p_2, \Omega) - Y_{12}(p_1, p_2, \Omega_B)), \quad (2.29)$$

where  $\Omega$  denotes the cut-off on the photon energies in either the rest frame of the decaying particle or the laboratory frame.

For consistency in defining the infrared region, in applying this weight we do not apply dipole weights for those photons whose energy is below the infrared cut-off.<sup>2</sup>

## 2.2 Initial-Final Dipole

In this subsection we describe our algorithm for dressing decays, in which a charged particle decays to another charged particle and a neutral particle. As in the final-final dipole case, the inputs to the algorithm are the momenta and quantum numbers of the parent particle and its children, distributed according to the leading-order differential decay rate.

The situation here is less complicated than for the final-final dipole case because we can use the neutral decay product to absorb the recoil due to the photonic radiation. This allows us to simulate the radiation in the rest frame of the decaying particle. As with the final-final dipole we must also rescale the three-momentum of the charged particle in order to have overall energy-momentum conservation.

---

<sup>2</sup>In practice if we neglect the mass terms when generating the crude distribution we also need to include the weight from (B.8) for the removed photons as part of the dipole weight in order to take this into account.

As in the previous subsection, we begin by manipulating the phase-space measure in order to factorize off a part of the integrand which can be interpreted as corresponding to the leading-order process. Taking  $p_1$  to be the momentum of the charged particle in the final state and integrating over the momentum  $|\vec{p}_1|$  and  $\vec{p}_2$ , in the rest frame of the decaying particle gives

$$\Gamma = \frac{1}{2M} \sum_{n_\gamma=0}^{\infty} \int d\Phi \frac{1}{n_\gamma!} e^{Y(p,p_1,\Omega)} \prod_{i=1}^{n_\gamma} \tilde{S}(p, p_1, k_i) \rho_{\alpha\beta} \mathcal{M}_\alpha \mathcal{M}_\beta^* \mathcal{C} \quad (2.30)$$

where

$$d\Phi = \frac{1}{4(2\pi)^2} d\Omega_{p_1} d\Phi_k \frac{|\vec{p}_1|^2}{p_1^0 \left( |\vec{p}_1| + |\vec{K}| \cos \theta_{p_1 K} \right) + p_2^0 |\vec{p}_1|}. \quad (2.31)$$

This can be rewritten as

$$\Gamma = \sum_{n_\gamma=0}^{\infty} \int d\Gamma_0 d\Phi_k \frac{|\vec{p}_1|^2 M}{|\vec{q}_1| p_1^0 \left( |\vec{p}_1| + |\vec{K}| \cos \theta \right) + |\vec{q}_1| p_2^0 |\vec{p}_1|} \frac{1}{n_\gamma!} e^{Y(p,p_1,\Omega)} \prod_{i=1}^{n_\gamma} \tilde{S}(p, p_1, k_i) \mathcal{C} \quad (2.32)$$

where

$$d\Gamma_0 = \frac{1}{2M} d\Omega_{q_1} \frac{|\vec{q}_1|}{4(2\pi)^2 M} \rho_{\alpha\beta} \mathcal{M}_\alpha \mathcal{M}_\beta^*. \quad (2.33)$$

As before, by not changing the angles of the photons with respect to the dipole (in this case the charged final-state particle) we have  $d\Omega_{p_1} = d\Omega_{q_1}$ . The generation of the leading-order process ( $d\Gamma_0$ ) may proceed prior to, and independently of, the details of QED radiation. That is to say that no changes need to be made to the existing decay program, the QED algorithm for initial-final dipoles is universal in this respect. Momentum conservation and on-shell conditions require that the momenta, after generation of the photons, are given by

$$\begin{aligned} p &= q, \\ p_1 &= \left( \sqrt{\rho^2 \vec{q}_1^2 + m_1^2}, \rho \vec{q}_1 \right), \\ p_2 &= \left( M - K_0 - \sqrt{\rho^2 \vec{q}_1^2 + m_1^2}, -\vec{K} - \rho \vec{q}_1 \right), \\ K &= \left( K_0, \vec{K} \right), \end{aligned} \quad (2.34)$$

where the rescaling factor  $\rho$  is

$$\rho = \frac{-|\vec{K}| \cos \theta_{1K} \left( (p_1 + p_2)^2 + m_1^2 - m_2^2 \right) + (M - K_0) \sqrt{\lambda \left( (p_1 + p_2)^2, m_1^2, m_2^2 \right) - 4m_1^2 K_\perp^2}}{2|\vec{q}_1| \left( (p_1 + p_2)^2 + K_\perp^2 \right)} \quad (2.35)$$

and  $K_\perp^2 = |\vec{K}|^2 \sin^2 \theta_{1K}$ .

The crude distribution, is obtained from the exact distribution (2.33) by dropping the kinematic factor arising from integrating over the delta function and the

higher-order non-soft photon corrections in  $\mathcal{C}$ . The momenta in the form factor and dipole functions are replaced by the values generated from the leading-order decay ( $\vec{q}_1 = -\vec{q}_2$ ) giving the crude distribution

$$\Gamma_{\text{crude}} = \sum_{n_\gamma=0}^{\infty} \int d\Gamma_0 d\Phi_k \frac{1}{n_\gamma!} e^{Y_{12}(q, q_1, \Omega)} \prod_{i=1}^{n_\gamma} \tilde{S}(q, q_1, k_i). \quad (2.36)$$

The dependence of QED part of (2.36) on the momenta  $q$  and  $q_1$  is overstated here, in the rest frame of the decaying particle the kinematics are so simple that this part only depends on the masses  $q^2$  and  $q_1^2$ . Therefore (2.36) is really a product of two independent integrals. The simplified kinematics allow the integral over the photon momenta to be performed analytically giving

$$\bar{n} = \int \frac{d^3 k_i}{k_i^0} \Theta(k_i, \Omega) \tilde{S}(q, q_1, k_i). \quad (2.37)$$

We therefore obtain

$$\Gamma_{\text{crude}} = \Gamma_0 \sum_{n_\gamma=0}^{\infty} \frac{1}{n_\gamma!} \bar{n}^{n_\gamma} e^{-\bar{n}} = \Gamma_0. \quad (2.38)$$

In obtaining this we have, as in the final-final dipole case, approximated  $Y \approx -\bar{n}$ . Once again we have reduced the width to a simple Poisson distribution for the photon multiplicity.

The generation of the crude width proceeds in the same way as for the final-final dipole. First we generate  $n_\gamma$  according to the Poisson distribution and then the photon momenta are generated according to the dipole functions (see Appendix B.1). The form of the rejection weights  $\mathcal{W}$  is similar to those in section 2.1 equation (2.27) with the following changes:

$$\begin{aligned} \mathcal{W}_{\text{dipole}} &= \prod_{i=1}^{n_\gamma} \frac{\tilde{S}(q, p_1, k_i)}{\tilde{S}(q, q_1, k_i)}, \\ \mathcal{W}_{\text{YFS}} &= \frac{e^{Y(q, p_1, \Omega)}}{e^{-\bar{n}}}, \\ \mathcal{W}_{\text{Jacobian}} &= \frac{|\vec{p}_1|^2 M}{p_1^0 (|\vec{p}_1| + |\vec{K}| \cos \theta) |\vec{q}_1| + p_2^0 |\vec{p}_1| |\vec{q}_1|}, \\ \mathcal{W}_{\text{higher}} &= \mathcal{C}. \end{aligned} \quad (2.39)$$

Unlike the case of the final-final dipole, we do not need a photon removal step because the decay is generated in the rest frame of the decaying particle.

### 3. Higher-Order Corrections

As stated in section 2, the effects of soft photons (photons with energy below the cut-off  $\omega$ ) have been included to all orders through the YFS form factor. If one neglects the infrared residuals in  $\mathcal{C}$ , the effect of the master formula and algorithms is, for a given multiplicity, to generate the QED radiation according to the dipole

radiation functions only. This amounts to approximating matrix elements for the decay  $p \rightarrow p_1 \dots p_n + n_\gamma \gamma$  by a product of eikonal factors multiplied by the leading-order matrix element. Ideally, we wish to include the higher-order effects in  $\mathcal{C}$  as far as possible.

Thus far our algorithms only require a set of momenta and their associated charges. Unfortunately calculating  $\mathcal{C}$  exactly to a given order in  $\alpha$  requires knowledge of the matrix elements for the specific decay process to that order. The structure of HERWIG++ is designed so that if these corrections are known they can be implemented. However, for the majority of decays these corrections will not be available and in this case we need to include the remaining enhanced contributions, *i.e.* the single collinear logarithmic terms. Depending on the mass scales involved, one can obtain a good approximation to  $\mathcal{C}$  by just including these leading mass singular terms.

In the collinear limit, the squared matrix element for a process including a massless emission, factorizes into the leading-order squared matrix element multiplied by a splitting function. The splitting functions only depend on the spin of the particles involved. Therefore if, in addition to the momenta and charges, we supply the program with the spins involved in the decay, we may include the leading non-soft, collinear logarithms in  $\mathcal{C}$  for the real emission contributions.

In addition to affording us a way to include higher-order hard emission contributions in a universal way, this approach has two further advantages. Firstly, as we shall describe in more detail in section 3.2, in this approach we can readily obtain a good approximation to the virtual corrections. Secondly, given the logarithms associated to the collinear emissions are universal, they are necessarily gauge invariant.

### 3.1 Real Emission Corrections: $\bar{\beta}_1^1$

In the quasi-collinear limit<sup>3</sup>, defined in [37], the matrix element including the emission of an additional collinear photon factorizes as

$$|\mathcal{M}_R^1|^2 \cong \sum_{i=1}^n \frac{e^2 Z_i^2}{p_i \cdot k} P_{ii} |\mathcal{M}|^2, \quad (3.1)$$

where  $\mathcal{M}$  is the matrix element for the leading-order process,  $|\mathcal{M}_R^1|^2$  is the spin-averaged matrix element with the inclusion of one additional photon,  $Z_i$  is the charge of the emitting particle,  $p_i$  is the momentum of the emitting particle and  $k$  is the momentum of the emitted photon.  $P_{ii}$  is the Altarelli-Parisi splitting function for emission of a photon from particle  $i$ , its form only depends on the spin of the emitting particle.

In [38] these splitting functions were used, together with the factorization of the matrix element in the soft limit, to construct so-called *dipole splitting functions* for

---

<sup>3</sup>The quasi-collinear limit is the generalisation of the usual collinear limit to the case where the emitting particle is massive.

massive particles. These terms have the correct behaviour in both the soft and quasi-collinear limits and smoothly interpolate between the two, *i.e.* they reproduce the massive splitting functions for (quasi-)collinear emissions and the soft photon, dipole, radiation functions for soft emissions. We choose to use dipole-like terms based on the expressions in [38], omitting some sub-leading terms which were included in [38] to allowed the functions to be analytically integrated over the phase space of the emitted photon. With the dipole subtraction terms we may write an approximation for the real emission matrix element

$$|\mathcal{M}_R^1|^2 \approx -e^2 \sum_{i<j}^n Z_i \theta_i Z_j \theta_j (\mathcal{D}_{ij} + \mathcal{D}_{ji}) |\mathcal{M}_n|^2, \quad (3.2)$$

where indices  $i$  and  $j$  refer to the two particles forming the electric dipole and we have applied the conservation of charge  $\sum_{i=0}^n \theta_i Z_i = 0$ .

We adopt the convention that the first index on  $\mathcal{D}_{ij}$  refers to the particle in the dipole which is considered to be emitting the photon, while the second index refers to the so-called *spectator* particle. From here we may write down a leading collinear approximation for the infrared finite residual  $\bar{\beta}_1^1$

$$\bar{\beta}_1^1 = -\frac{\alpha}{4\pi^2} \rho_{\alpha\beta} \mathcal{M}_\alpha \mathcal{M}_\beta^* \sum_{i<j}^n Z_i \theta_i Z_j \theta_j [\bar{\mathcal{D}}_{ij} + \bar{\mathcal{D}}_{ji}], \quad (3.3)$$

where the  $\bar{\mathcal{D}}_{ij}$  are the infrared subtracted counterparts of  $\mathcal{D}_{ij}$ ,

$$\bar{\mathcal{D}}_{ij} = \mathcal{D}_{ij} - \frac{1}{p_i \cdot k} \left[ \frac{2p_i \cdot p_j}{(p_i + p_j) \cdot k} - \frac{m_i^2}{(p_i \cdot k)} \right]. \quad (3.4)$$

For the case that both the emitter and spectator are in the final state, the dipole terms are given by<sup>4</sup>

$$\begin{aligned} \mathcal{D}_{ij} &= \frac{1}{p_i \cdot k} \left[ \frac{2p_i \cdot p_j}{(p_i + p_j) \cdot k} - \frac{m_i^2}{p_i \cdot k} \right] && \text{spin } 0, \\ &= \frac{1}{p_i \cdot k} \left[ \frac{p_j \cdot k}{(p_i + k) \cdot p_j} + \frac{2p_i \cdot p_j}{(p_i + p_j) \cdot k} - \frac{m_i^2}{p_i \cdot k} \right] && \text{spin } \frac{1}{2}, \\ &= \frac{1}{p_i \cdot k} \left[ \frac{2(p_j \cdot k)(p_i \cdot p_j)}{((p_i + k) \cdot p_j)^2} + \frac{2p_j \cdot k}{(p_j + k) \cdot p_i} + \frac{2p_i \cdot p_j}{(p_i + p_j) \cdot k} - \frac{m_i^2}{p_i \cdot k} \right] && \text{spin } 1. \end{aligned} \quad (3.5)$$

For the case that the dipole is comprised of the decaying particle (which we shall denote by index  $j$ ) and one of its children, the  $\mathcal{D}_{ij}$  functions for emissions from the children are taken to be the same as in (3.5). However, for the decaying particle, we assume that it is sufficiently massive for us to neglect collinear enhancements, giving the following dipole function

$$\mathcal{D}_{ji} = \frac{1}{p_j \cdot k} \left[ \frac{2p_i \cdot p_j}{(p_i + p_j) \cdot k} - \frac{m_j^2}{p_j \cdot k} \right] \text{spin } 0, \frac{1}{2}, 1. \quad (3.6)$$

---

<sup>4</sup>It is not possible to construct a quasi-collinear limit for the spin-1 splitting function, for a massive vector particle, in which the massless limit can be taken. We therefore use the corresponding expression for the massless dipole splitting function, augmented by a mass term which produces the correct behaviour in the soft limit.



Since the effects of collinear radiation from the decaying particle are neglected, only soft emissions are taken into account and so this dipole function is independent of the particle's spin. Furthermore, the infrared subtracted dipole splitting function, with the parent particle as the emitter, is identically zero:  $\bar{\mathcal{D}}_{ji} \equiv 0$ .

In the soft limit these expressions reproduce the expected eikonal result

$$\mathcal{D}_{ij} + \mathcal{D}_{ji} = - \left( \frac{p_i}{p_i \cdot k} - \frac{p_j}{p_j \cdot k} \right)^2 \quad (3.7)$$

and in the collinear limit the  $\mathcal{D}_{ij}$  equals the quasi-collinear splitting functions given in [37].

### 3.2 Virtual Corrections: $\bar{\beta}_0^1$

At present we have only implemented virtual corrections for two special cases in the SOPHTY code, those of initial-final and final-final dipoles with (relativistic) fermions in the final state, as in W and Z boson decays. These corrections turn out to have a negligible effect on *distributions*, compared to those of the real corrections. This is seen to be the case even for  $W \rightarrow e^+ \nu_e$  and  $Z \rightarrow e^+ e^-$  decays where one expects such effects to be greatest.

As with the real emission we try to work in a universal way, without referring to the details of the matrix elements, using the leading log approximation.

For both the case of the final-final dipole and the initial-final dipole the relevant virtual processes are represented by the lowest-order diagram with a photon joining the dipole constituents. On dimensional grounds, the large, leading logarithms of QED will be logarithms of  $M^2/m_i^2$ . Also, if we regularize the infrared divergences by introducing a fictitious photon mass  $m_\gamma$ , logarithms of  $M^2/m_\gamma^2$  and  $m_i^2/m_\gamma^2$  are possible.

The infrared divergences from virtual corrections, must cancel the infrared divergences arising from the soft region of the photon phase space in the real emission process [39]. Likewise, terms diverging as  $m_i^2 \rightarrow 0$ , so called *mass/collinear divergences*, must also cancel between the real emission corrections and their virtual counterparts, this is the KLN theorem [40, 41]. Using the fact that the  $m_\gamma \rightarrow 0$  and  $m_i^2 \rightarrow 0$  divergent logarithms have to cancel in this way, we can construct the leading log approximation to the loop integrals.

To obtain the leading soft and collinear contributions to the virtual terms we therefore return to the soft and collinear approximation that was used for the real emission matrix element (3.2). We calculate the leading logarithms arising in the real emission contribution by integrating the full dipole function over the *full* phase space for the emission of the photon *i.e.* both the soft  $k_0 < \omega$  and hard  $k_0 \geq \omega$  regions as was done in [38]. Performing the relevant integrals and taking the small

mass limit gives the contribution of the virtual terms for the different types of dipole

$$\begin{aligned} d\Gamma|_{\text{LL}} &= \frac{\alpha}{\pi} \left( 2 \left( \ln \left( \frac{M}{m_i} \right) - 1 \right) \ln \left( \frac{m_\gamma}{M} \right) + \ln^2 \left( \frac{M}{m_i} \right) + \frac{1}{2} \ln \left( \frac{M}{m_i} \right) \right) d\Gamma_0 \quad (\text{initial-final}), \\ d\Gamma|_{\text{LL}} &= \frac{\alpha}{\pi} \left( 2 \left( \ln \left( \frac{M^2}{m_i^2} \right) - 1 \right) \ln \left( \frac{m_\gamma}{M} \right) + \frac{1}{2} \ln^2 \left( \frac{M^2}{m_i^2} \right) + \frac{1}{2} \ln \left( \frac{M^2}{m_i^2} \right) \right) d\Gamma_0 \quad (\text{final-final}). \end{aligned} \quad (3.8)$$

These expressions agree, at the level of large logarithms, with those obtained by direct calculation in [42] and [17]. From here we see that the  $\bar{\beta}_0^1$  functions we require are, for the initial-final dipole

$$\bar{\beta}_0^1 = \frac{\alpha}{2\pi} \ln \left( \frac{M^2}{m_i^2} \right) \bar{\beta}_0^0, \quad (3.9)$$

and for the final-final dipole,

$$\bar{\beta}_0^1 = \frac{\alpha}{\pi} \ln \left( \frac{M^2}{m_i^2} \right) \bar{\beta}_0^0. \quad (3.10)$$

For resonant  $Z \rightarrow e^+e^-$  processes this number is around 6%, dropping to around 3% for resonant  $Z \rightarrow \mu^+\mu^-$  processes. The extension to other cases is obvious, it simply requires the use of the scalar and vector splitting functions instead.

## 4. Results

In this section we discuss the results from the SOPHTY program as implemented in HERWIG++. In order to test the algorithm we will consider both leptonic  $Z$  and  $W$  boson decays, due to their phenomenological importance. In addition we will consider a number of important meson decays to demonstrate the application of the program to hadronic decays. We reiterate that our approach simulates the soft photon corrections in the leading log approximation which depends on nothing more than the momenta and charges of the primary decay products, and simulation of hard collinear photons merely requires additional spin information. This being the case these examples represent a general test of our methods.

The key distribution produced by the simulation is the total photon energy spectrum ( $K_0$ ). This is shown for  $Z$  decays in figure 1 and for  $W$  decays in figure 2. We have considered a large range of masses for the decay products, including a fictitious heavy lepton ( $\tau'$ ), to check for numerical instabilities and other irregular behaviour. For each type of decay we show the results of our algorithm including only soft photon effects and also with the dipole approximation for hard radiation. In all cases the amount of radiation is seen to decrease smoothly as the mass of the decay products increases, this can be understood from simple phase-space considerations.

One can also see that the inclusion of the dipole splitting functions ( $\mathcal{D}_{ij}$ ) leads to an enhancement of hard photon radiation. This enhancement is most prominent

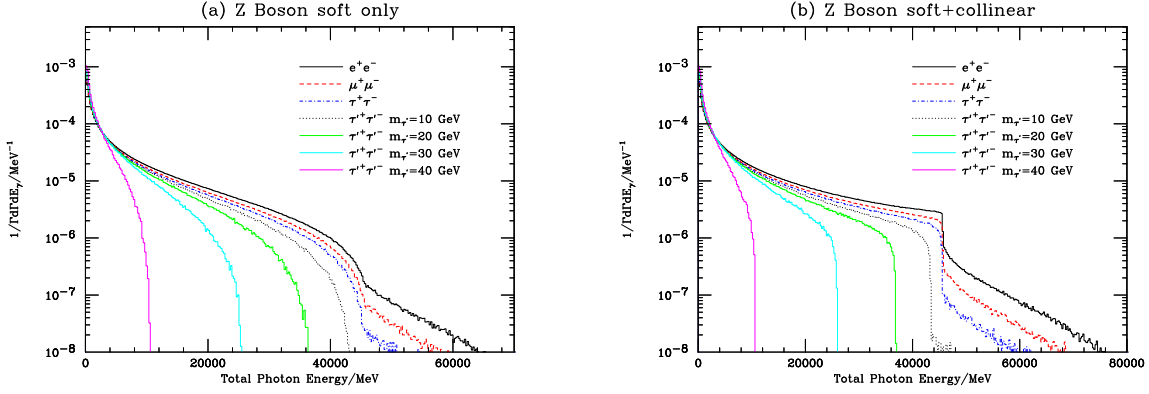


**Figure 1:** The total energy ( $K_0$ ) of the photons radiated in Z boson decays to leptons: (a) shows the  $K_0$  spectrum for the case that no infrared residuals are considered ( $\mathcal{C} = 1$ ); (b) shows the effect of including the collinear approximation for the  $\mathcal{O}(\alpha)$  residual  $\bar{\beta}_1^1$ .

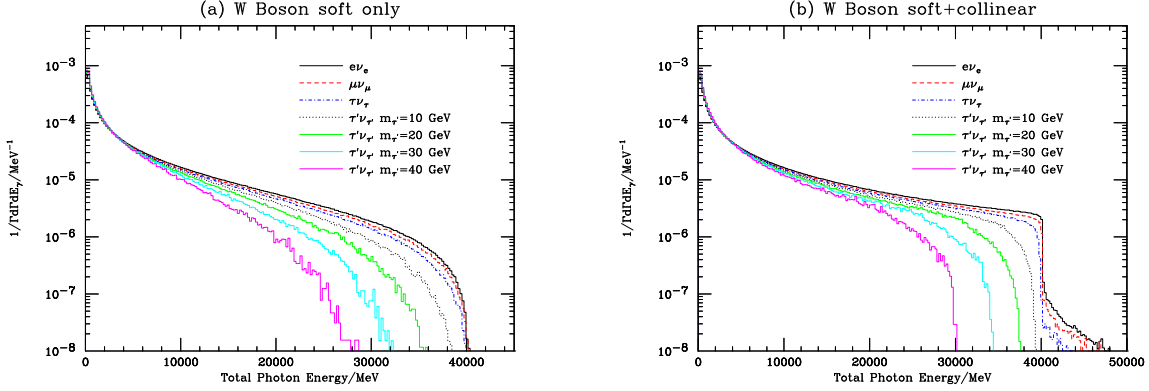


**Figure 2:** The total energy ( $K_0$ ) of the photons radiated in W boson decays to leptons; (a) shows the  $K_0$  spectrum for the case that no infrared residuals are considered ( $\mathcal{C} = 1$ ); (b) shows the effect of including the collinear approximation for the  $\mathcal{O}(\alpha)$  residual  $\bar{\beta}_1^1$ .

for lighter decay products, for the heavier decay products the effect is negligible. Again, this is to be expected as the mass of the emitting particle is known to screen the collinear divergence, this can be seen by considering, for instance, the massive splitting functions in [37].

Including the hard collinear enhancements also reveals a kink in the total photon energy spectrum. This kink occurs at a kinematic endpoint, beyond it all events must contain at least two photons which recoil against each other, hence the histograms drop beyond this value. Looking in this two photon region we also see that the photon multiplicity increases as the mass of the primary decay products decreases.

Changing the spin of the primary decay products does not affect the soft distributions in figures 1a and 2a, it does however, influence the other distributions where hard collinear photon effects are introduced. The program uses the other splitting functions in (3.5) to account for this, although in the case that the decaying particle

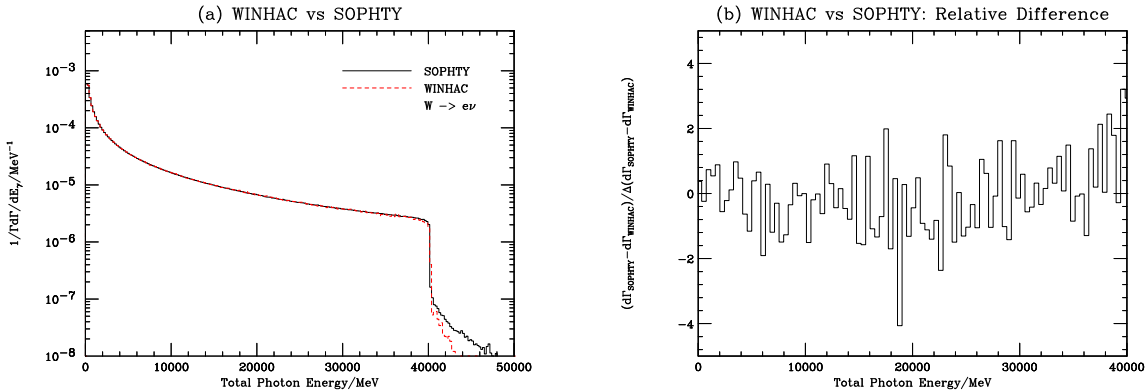


**Figure 3:** The total energy ( $K_0$ ) of the photons radiated in  $W^\pm \rightarrow e^\pm \nu_e / \bar{\nu}_e$  decays. In figure (a) the red histogram was generated using the WINHAC [21] simulation, including exact  $\mathcal{O}(\alpha)$  real emission corrections to the  $W^\pm$  decay, while the black line was generated using the SOPHTY module for QED radiation in HERWIG++. In figure (b) we show the difference between the spectra shown in (a) divided by the associated statistical error. The discrepancy in the region beyond 40 GeV is exclusively comprised of events with at least two non-soft photons, which neither program is designed to model well.

is a scalar there will be no collinear enhancement since in this case  $\bar{\mathcal{D}}_{ij} \equiv 0$ .

In figure 3 we compare the total photon energy spectrum for  $W \rightarrow e \nu_e$  decays as generated by our program and that of the WINHAC generator. The agreement is seen to be quite good except in the region beyond the kink at around 40 GeV. As mentioned earlier, this region is populated exclusively by events with at least two hard photons. Consequently neither simulation expects to model this accurately. A correct modelling of this region will require the calculation of the infrared residuals ( $\mathcal{C}$ ) to  $\mathcal{O}(\alpha^2)$ . This extension may be implemented in future versions of the program. We note that WINHAC was been independently compared with another simulation of the charged Drell-Yan process, HORACE, in [43], where good numerical agreement between the different approaches to QED radiation was recorded.

The total energy of the photons radiated in the decays of some neutral vector mesons is shown in figure 4. Here we see that the energy distribution shows a behaviour that qualitatively resembles that seen in the case of the  $Z$  boson. In this case, as the decay products are pseudoscalar mesons, there is no effect from including the collinear approximation for the radiation. In addition figure 4c shows the radiation for an example,  $K^{*0} \rightarrow K^\pm \pi^\mp$ , with unequal masses for the decay products. Here we see that the lighter decay product is responsible for the more energetic photons, as we increase its mass (for illustrative purposes) the distribution tends toward lower energies.

The total energy of the photonic radiation in the decays of some charged vector mesons is shown in figure 5. As expected, for these decays the distributions be-

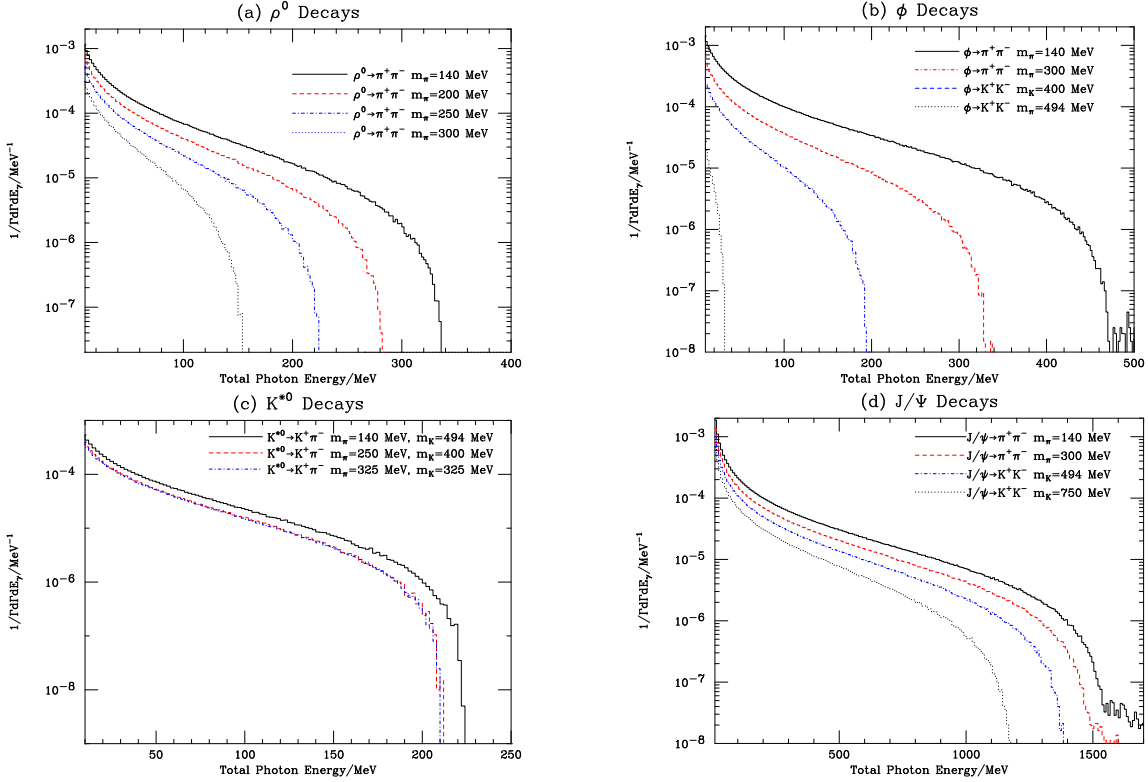


**Figure 4:** The total energy ( $K_0$ ) of the photons radiated in the decays of neutral vector mesons to pseudoscalar mesons for a number of different decays: (a)  $\rho \rightarrow \pi^+\pi^-$ ; (b)  $\phi \rightarrow \pi^+\pi^-$  and  $\phi \rightarrow K^+K^-$ ; (c)  $K^{*0} \rightarrow K^\pm\pi^\mp$ ; (d)  $J/\psi \rightarrow \pi^+\pi^-$  and  $J/\psi \rightarrow K^+K^-$ . In addition to using the real physical masses of the decay products we have included the effect of varying the masses of the decay products.

have in a similar way to those of the W boson, since they involve the same type of dipole. As with the neutral vector meson decays there is no effect from including the collinear approximation for the photon radiation as the decay products are pseudoscalar mesons ( $\bar{D}_{ij} \equiv 0$ ). The  $K^{*\pm}$  decays show the effect of having unequal mass decay products.

For the leptonic decays of the charmonium resonances and the  $\Upsilon$  resonance, the total energy spectrum of the radiated photons is shown in figures 6 and 7 respectively. As for Z decays, the effects of varying the  $\tau$  mass are included to show the mass dependence of the results. In the charmonium decays to  $\tau^+\tau^-$  pairs we see a suppression of QED radiation since these decay modes are near the production threshold; for the physical  $\tau$  mass, this decay mode is not accessible in  $J/\psi$  decays, while for  $\psi(2s)$  and  $\psi(3770)$  it is just below the threshold. The  $\Upsilon$  resonance is significantly more massive and therefore the associated photon energy spectrum more closely resembles that seen for the case of the Z boson.

These results show that the approach can be successfully applied to both per-

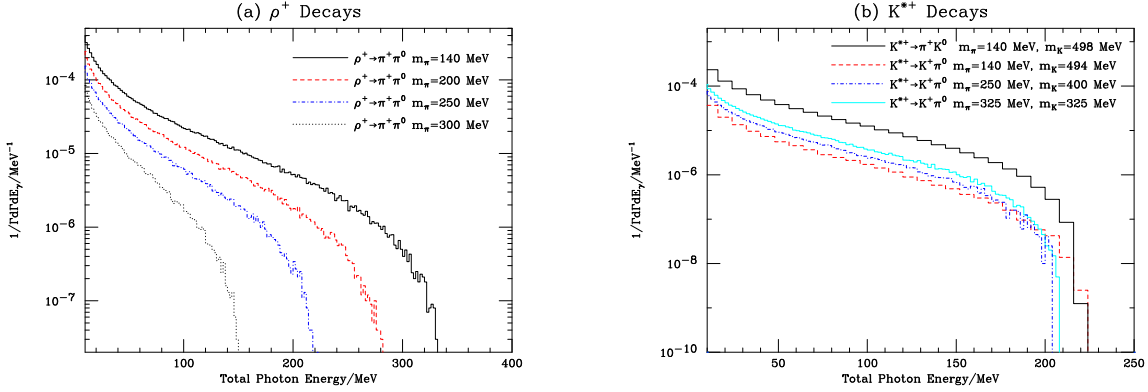


**Figure 5:** The total energy ( $K_0$ ) of the photons radiated in the decays of charged vector mesons to pseudoscalar mesons for the decays: (a)  $\rho^\pm \rightarrow \pi^\pm \pi^0$ ; (b)  $K^{*\pm} \rightarrow K^\pm \pi^0$  and  $K^{*\pm} \rightarrow K^0 \pi^\pm$ . In addition to using the real physical masses of the decay products we have included the effect of varying the masses of the decay products.

turbative decays and non-perturbative hadronic decays.

## 5. Conclusions

In this paper we have presented a universal theoretical framework for calculating QED radiative corrections to particle decays based on the YFS formalism [15] and the methods of [17, 18, 33]. The essence of this approach is a reorganization of the perturbation series to resum all soft divergent QED logarithms. This formalism led to the master formula presented in (2.3).

The master formula forms the basis of the Monte Carlo event generator SOPHTY, which provides QED radiative corrections for decays inside the HERWIG++ generator. The Monte Carlo simulation takes into account large soft photon logarithms to all orders. In addition, the leading collinear logarithms are included to  $\mathcal{O}(\alpha)$  by using the so-called dipole splitting functions and inferring the associated virtual corrections with the aid of the Bloch-Nordsieck and the KLN theorems.

Algorithms for the two basic “building-block” cases of dipoles comprising either two final-state particles, or the initial-state particle and one of its decay products, are presented in section 2. Although integrals like that of the master equation can generally be readily performed with conventional Monte Carlo methods to give weighted events, the manipulations required in order to produce unweighted events with good efficiency (*i.e.* an event generator) are non-trivial.

In designing these algorithms we were constrained by the requirement that the QED radiation should be generated, as far as possible, independently of the details of the main HERWIG++ program, which should provide the initial distribution of decay products. This was made possible due to the form of the master equation,

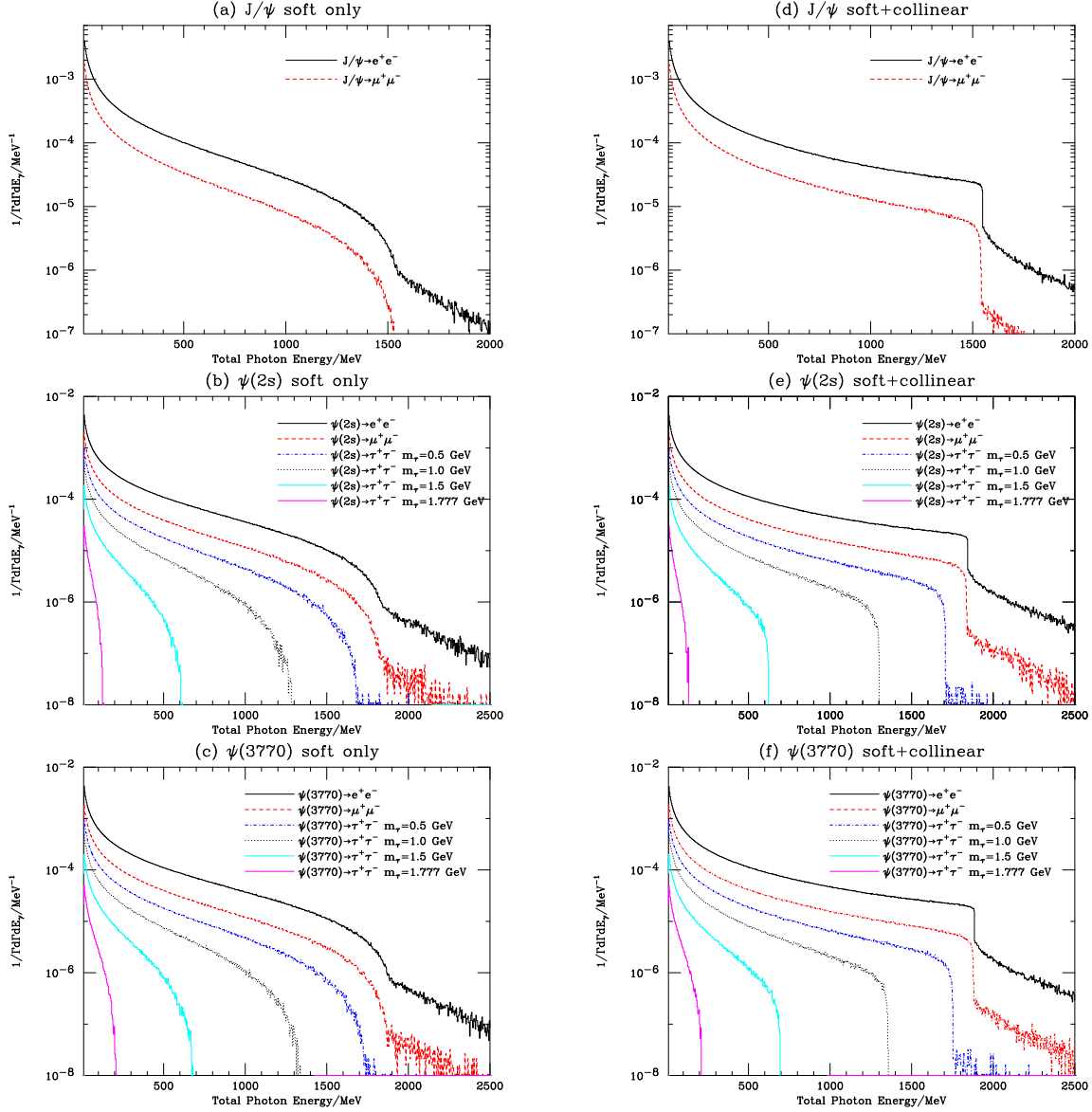


**Figure 6:** The total energy ( $K_0$ ) of the photons radiated in leptonic decays of charmonium resonances is shown above for  $J/\psi$  (a/d),  $\psi(2s)$  (b/e) and  $\psi(3770)$  (c/f). The distributions on the left, figures (a), (b) and (c), are obtained by truncating the infrared residuals at  $\mathcal{O}(1)$ , whereas in (d), (e) and (f), the dipole splitting functions are used to include the effects of hard collinear photons. In addition to the real charged leptons we have included the effect of varying the  $\tau$  mass to illustrate the mass dependence of the results.

the universal nature of the radiative corrections involved and our simplified crude distribution from which we initially generate the photons. Care was taken to design the algorithms to keep event weights as close to one as possible and to avoid numerical instabilities. Key to realising these features are importance sampling techniques and, importantly, a careful choice of frame in which to generate the radiation.

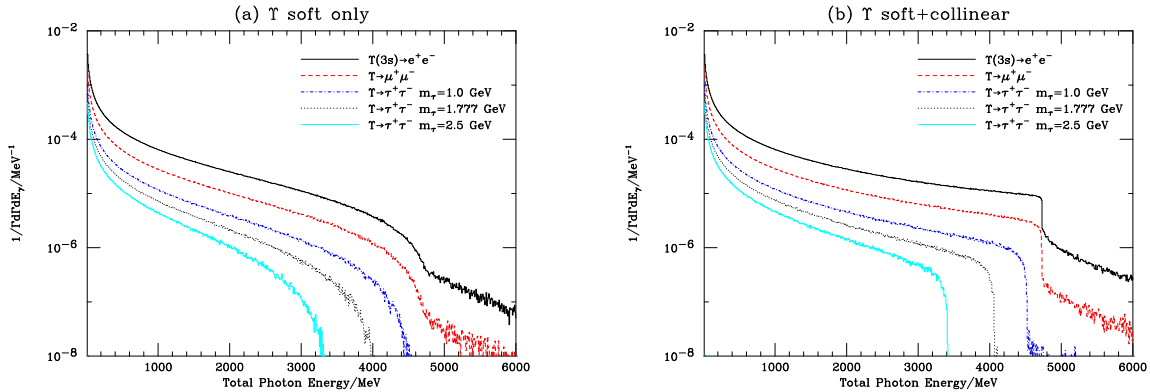


**Figure 7:** The total energy ( $K_0$ ) of the photons radiated in leptonic decays of the bottomonium resonance  $\Upsilon$ . The distribution on the left (a) is obtained by truncating the infrared residuals at  $\mathcal{O}(1)$ , whereas in (b), the dipole splitting functions ( $\mathcal{D}_{ij}$ ) are used to include the effects of hard collinear emissions.

Our algorithm was tested successfully for several different types of particle decay produced by the HERWIG++ generator. In section 4 we have shown results for the important cases of W and Z decays to various lepton species. In all cases the distributions show a smooth and stable behaviour agreeing with our expectations. A preliminary comparison of the total photon energy spectrum from the WINHAC generator shows good agreement and provides a good check of our methods. The application of the program to both hadronic and leptonic meson decays was also illustrated in section 4.

There are several possible extensions of this work, for instance, there are a number phenomenologically important decays for which the full  $\mathcal{O}(\alpha)$  corrections are known *e.g.* W and Z decays. As the code is designed to readily allow these corrections to be included they will be implemented in the near future. In addition, there are a small number of cases inside the HERWIG++ where we have to simulate multi (*i.e.* greater than two) body decays and the extension of the algorithm to these cases would be useful. This is the first use of the YFS approach within the HERWIG++ program and there are a number of other potential applications, for example initial-state radiation in lepton collisions, which may be pursued in the future.

In conclusion, we have applied the YFS formalism to the simulation of QED radiation in particle decays. The simulation, SOPHTY, based on the results of this work can simulate QED radiation in a wide range of particle decays and will be available in the next version of the HERWIG++ program.



## Acknowledgements

We would like to thank our collaborators on the HERWIG++ project for many fruitful discussions. This work was supported by PPARC.

## A. YFS Form Factors

In this appendix we give the expressions we calculate for the YFS form factors. For both the final-final dipole form factor and the initial-final dipole form factor we use,  $\beta_i = |\vec{p}_i|/E_i$ , to denote the velocity of particle  $i$ . Furthermore, in each case we have assumed that the momenta obey  $p = p_1 + p_2$ .

### A.1 Final-Final Dipoles

Below in (A.1) we have the YFS form factor for a pair of final state charged particles with momenta  $p_1, p_2$  whose combined momentum is  $p$ . Expression (A.1) is valid in the frame  $\vec{p}_1 = -\vec{p}_2$ .

$$\begin{aligned}
Y(p_1, p_2, \Omega) &= -\frac{\alpha}{2\pi} Z_1 Z_2 \hat{Y}(p_1, p_2, \Omega) \\
\hat{Y}(p_1, p_2, \Omega) &= \left(4 - 2 \left(\frac{1+\beta_1\beta_2}{\beta_1+\beta_2}\right) \left(\ln\left(\frac{1+\beta_1}{1-\beta_1}\right) + \ln\left(\frac{1+\beta_2}{1-\beta_2}\right)\right)\right) \ln\left(\frac{\sqrt{p^2}}{2\omega}\right) \\
&\quad - \frac{1}{2} \ln\left(\frac{p^2}{p_1^2}\right) - \frac{1}{2} \ln\left(\frac{p^2}{p_2^2}\right) - 2 \\
&\quad + \left(\frac{\beta_2-\beta_1\beta_2}{\beta_1+\beta_2}\right) \ln\left(\frac{\beta_2-\beta_1\beta_2}{\beta_1+\beta_2}\right) + \left(\frac{\beta_1+\beta_1\beta_2}{\beta_1+\beta_2}\right) \ln\left(\frac{\beta_1+\beta_1\beta_2}{\beta_1+\beta_2}\right) \\
&\quad + \left(\frac{\beta_1-\beta_1\beta_2}{\beta_1+\beta_2}\right) \ln\left(\frac{\beta_1-\beta_1\beta_2}{\beta_1+\beta_2}\right) + \left(\frac{\beta_2+\beta_1\beta_2}{\beta_1+\beta_2}\right) \ln\left(\frac{\beta_2+\beta_1\beta_2}{\beta_1+\beta_2}\right) \\
&\quad + \frac{1+\beta_1\beta_2}{\beta_1+\beta_2} \left(\frac{1}{2} \ln^2\left(\frac{\beta_2-\beta_1\beta_2}{\beta_1+\beta_2}\right) - \frac{1}{2} \ln^2\left(\frac{\beta_2+\beta_1\beta_2}{\beta_1+\beta_2}\right)\right) \\
&\quad + \frac{1+\beta_1\beta_2}{\beta_1+\beta_2} \left(\frac{1}{2} \ln^2\left(\frac{\beta_1-\beta_1\beta_2}{\beta_1+\beta_2}\right) - \frac{1}{2} \ln^2\left(\frac{\beta_1+\beta_1\beta_2}{\beta_1+\beta_2}\right)\right) \\
&\quad - \frac{1+\beta_1\beta_2}{\beta_1+\beta_2} \left(2\text{Li}_2\left(-\frac{1-\beta_1}{2\beta_1}\right) + 2\text{Li}_2\left(-\frac{1-\beta_2}{2\beta_2}\right)\right) \\
&\quad - \frac{1+\beta_1\beta_2}{\beta_1+\beta_2} \left(2\text{Li}_2\left(\frac{2\beta_1}{1+\beta_1}\right) + 2\text{Li}_2\left(\frac{2\beta_2}{1+\beta_2}\right)\right) \\
&\quad - \frac{1+\beta_1\beta_2}{\beta_1+\beta_2} \left(\ln\left(\frac{1-\beta_1}{2\beta_1}\right) \ln\left(\frac{1+\beta_1}{2\beta_1}\right) + \ln\left(\frac{1-\beta_2}{2\beta_2}\right) \ln\left(\frac{1+\beta_2}{2\beta_2}\right)\right) \\
&\quad + \frac{1+\beta_1\beta_2}{\beta_1+\beta_2} \ln\left(\frac{2\beta_1\beta_2}{\beta_1+\beta_2}\right) \left(\ln\left(\frac{\beta_2-\beta_1\beta_2}{\beta_1+\beta_2}\right) - \ln\left(\frac{\beta_2+\beta_1\beta_2}{\beta_1+\beta_2}\right)\right) \\
&\quad + \frac{1+\beta_1\beta_2}{\beta_1+\beta_2} \ln\left(\frac{2\beta_1\beta_2}{\beta_1+\beta_2}\right) \left(\ln\left(\frac{\beta_1-\beta_1\beta_2}{\beta_1+\beta_2}\right) - \ln\left(\frac{\beta_1+\beta_1\beta_2}{\beta_1+\beta_2}\right)\right) \\
&\quad + \frac{1+\beta_1\beta_2}{\beta_1+\beta_2} \left(\frac{4\pi^2}{3}\right) - \frac{1}{\beta_1} \ln\left(\frac{1-\beta_1}{1+\beta_1}\right) - \frac{1}{\beta_2} \ln\left(\frac{1-\beta_2}{1+\beta_2}\right) \\
&\quad - \frac{1+\beta_1\beta_2}{\beta_1+\beta_2} \left(\frac{1}{2} \ln^2\left(\frac{1-\beta_1}{1+\beta_1}\right) + \frac{1}{2} \ln^2\left(\frac{1-\beta_2}{1+\beta_2}\right)\right)
\end{aligned} \tag{A.1}$$

We have checked that for the case  $\beta_1 = \beta_2$ , in the limit  $\beta_1 \rightarrow 1$ , expression (A.1) reduces to

$$Y(p_1, p_2, \Omega) = -\frac{\alpha}{\pi} Z_1 Z_2 \left(2 \ln\left(\frac{2\omega}{\sqrt{p^2}}\right) \left(\ln\left(\frac{p^2}{p_1^2}\right) - 1\right) + \frac{1}{2} \ln\left(\frac{p^2}{p_1^2}\right) - 1 + \frac{\pi^2}{3}\right), \tag{A.2}$$

in agreement with the previously obtained results [19].

## A.2 Initial-Final Dipoles

In equation (A.3) we have the YFS form factor for a pair of charged particles of momentum  $p$  and  $p_1$ , ( $p_2 = p - p_1$ ), evaluated in the rest frame of  $p$ .

$$\begin{aligned}
Y(p, p_1, \Omega) &= \frac{\alpha}{2\pi} Z_p Z_1 \hat{Y}(p, p_1, \Omega) \\
\hat{Y}(p, p_1, \Omega) &= \ln\left(\frac{p^2}{4\omega^2}\right) + \ln\left(\frac{p_1^2}{4\omega^2}\right) - \frac{1}{\beta_1} \ln\left(\frac{1+\beta_1}{1-\beta_1}\right) \ln\left(\frac{p_2^2}{4\omega^2}\right) \\
&\quad + \frac{1}{2} \ln\left(\frac{p_2^4}{p^2 p_1^2}\right) - \frac{1}{\beta_1} \ln\left(\frac{1-\beta_1}{1+\beta_1}\right) - \frac{1}{2\beta_1} \ln^2\left(\frac{1-\beta_1}{1+\beta_1}\right) \\
&\quad + \left(\frac{\beta_1+\beta_2}{\beta_1-\beta_1\beta_2}\right) \ln\left(\frac{\beta_1+\beta_2}{\beta_1-\beta_1\beta_2}\right) - \left(\frac{\beta_2+\beta_1\beta_2}{\beta_1-\beta_1\beta_2}\right) \ln\left(\frac{\beta_2+\beta_1\beta_2}{\beta_1-\beta_1\beta_2}\right) \\
&\quad + \left(\frac{\beta_1+\beta_2}{\beta_1+\beta_1\beta_2}\right) \ln\left(\frac{\beta_1+\beta_2}{\beta_1+\beta_1\beta_2}\right) - \left(\frac{\beta_2-\beta_1\beta_2}{\beta_1+\beta_1\beta_2}\right) \ln\left(\frac{\beta_2-\beta_1\beta_2}{\beta_1+\beta_1\beta_2}\right) \\
&\quad + \frac{1}{2\beta_1} \ln^2\left(\frac{\beta_1+\beta_2}{\beta_1-\beta_1\beta_2}\right) - \frac{1}{2\beta_1} \ln^2\left(\frac{\beta_2+\beta_1\beta_2}{\beta_1-\beta_1\beta_2}\right) \\
&\quad + \frac{1}{2\beta_1} \ln^2\left(\frac{\beta_2-\beta_1\beta_2}{\beta_1+\beta_1\beta_2}\right) - \frac{1}{2\beta_1} \ln^2\left(\frac{\beta_1+\beta_2}{\beta_1+\beta_1\beta_2}\right) \\
&\quad + \frac{2}{\beta_1} \text{Li}_2\left(-\frac{1-\beta_2}{2\beta_2}\right) - \frac{2}{\beta_1} \text{Li}_2\left(-\frac{(1-\beta_1)(1-\beta_2)}{2(\beta_1+\beta_2)}\right) - \frac{2}{\beta_1} \text{Li}_2\left(\frac{2\beta_1}{1+\beta_1}\right) \\
&\quad + \frac{1}{\beta_1} \ln\left(\frac{\beta_1+\beta_2}{\beta_1+\beta_1\beta_2}\right) \ln\left(\frac{1+\beta_2}{2\beta_2}\right) - \frac{1}{\beta_1} \ln\left(\frac{\beta_2(1-\beta_1)}{\beta_1(1+\beta_2)}\right) \ln\left(\frac{(1+\beta_1)(1+\beta_2)}{2(\beta_1+\beta_2)}\right) \\
&\quad - \frac{1}{\beta_1} \ln\left(\frac{2\beta_2}{\beta_1} \left(\frac{\beta_1+\beta_2}{1-\beta_2^2}\right)\right) \ln\left(\frac{\beta_1+\beta_2}{\beta_2-\beta_1\beta_2}\right).
\end{aligned} \tag{A.3}$$

We use  $Z_p$  to denote the charge on the particle with momentum  $p$ . For the special case that  $(p - p_2)^2$  is zero, as in leptonic  $W^\pm$  decay with a massless neutrino, we use the a more specialized compact form, to avoid potential numerical problems:

$$\begin{aligned}
Y(p, p_1, \Omega) &= \frac{\alpha}{2\pi} Z_p Z_1 Y(p, p_1, \Omega) \\
\hat{Y}(p, p_1, \Omega) &= \ln\left(\frac{p^2}{4\omega^2}\right) + \ln\left(\frac{p_1^2}{4\omega^2}\right) - \frac{1}{\beta_1} \ln\left(\frac{1+\beta_1}{1-\beta_1}\right) \ln\left(\frac{p^2-p_1^2}{4\omega^2}\right) - \frac{1}{2} \ln\left(\frac{1-\beta_1^2}{4\beta_1^2}\right) \\
&\quad + \left(\frac{1+\beta_1}{2\beta_1}\right) \ln\left(\frac{1+\beta_1}{2\beta_1}\right) - \left(\frac{1-\beta_1}{2\beta_1}\right) \ln\left(\frac{1-\beta_1}{2\beta_1}\right) - \frac{1}{\beta_1} \ln\left(\frac{1-\beta_1}{1+\beta_1}\right) + 1 \\
&\quad + \frac{1}{2\beta_1} \ln^2\left(\frac{1-\beta_1}{2\beta_1}\right) - \frac{1}{2\beta_1} \ln^2\left(\frac{1+\beta_1}{2\beta_1}\right) - \frac{1}{2\beta_1} \ln^2\left(\frac{1-\beta_1}{1+\beta_1}\right) - \frac{2}{\beta_1} \text{Li}_2\left(\frac{2\beta_1}{1+\beta_1}\right).
\end{aligned} \tag{A.4}$$

We have checked, analytically, that in the limit  $\beta_2 \rightarrow 1$  the virtual contributions ( $\mathcal{R}e B(p, p_1)$ ) to  $Y(p, p_1, \Omega)$  inside (A.3) are equal to those in (A.4). In both cases the real contributions are identical, they do not involve  $\beta_2$ , naturally as these contributions should only involve the moving charge in the dipole. Finally, as a check we observe that, dropping terms smaller than  $\mathcal{O}(p_1^2/p^2)$  the form factor (A.4) agrees exactly with the corresponding expression in [21].

## B. Generation of the Dipole Distributions

In this appendix we describe how to generate the photon momenta from the dipole radiation functions.

## B.1 Final-Final Dipoles

Consider the integral of the dipole function in the rest frame of  $p_1 + p_2$

$$\int \frac{d^3k}{k_0} \tilde{S}(p_1, p_2, k) = \frac{\alpha}{4\pi^2} Z_1 Z_2 \int dc d\phi dk_0 k_0 \left( \frac{p_1}{p_1 \cdot k} - \frac{p_2}{p_2 \cdot k} \right)^2. \quad (\text{B.1})$$

We choose to define the photon momenta as being with respect to  $p_1$ , with  $c \equiv \cos \theta$  *i.e.*

$$\begin{aligned} p_1 \cdot k &= E_1 k_0 (1 - \beta_1 c), \\ p_2 \cdot k &= E_2 k_0 (1 + \beta_2 c). \end{aligned} \quad (\text{B.2})$$

Using this representation of the momenta the integral can be rewritten as

$$\int \frac{d^3k}{k_0} \tilde{S}(p_1, p_2, k) = -\frac{\alpha}{4\pi^2} Z_1 Z_2 \int dc d\phi d \ln k_0 \left( -\frac{1-\beta_1^2}{(1-\beta_1 c)^2} + \frac{2(1+\beta_1 \beta_2)}{(1-\beta_1 c)(1+\beta_2 c)} - \frac{1-\beta_2^2}{(1+\beta_2 c)^2} \right). \quad (\text{B.3})$$

The photon momenta can be generated according to this distribution in the following way.

1. First the magnitude of the photon's momentum is generated logarithmically between  $\omega$ , the minimum photon energy cut-off, and the maximum possible photon energy,  $E_{\max}$ , *i.e.*

$$k_0 = \omega \left( \frac{E_{\max}}{\omega} \right)^{\mathcal{R}}, \quad (\text{B.4})$$

where  $\mathcal{R}$  is a random number uniformly distributed between 0 and 1. As the photon momenta are generated in the rest frame of the dipole the maximum energy of the photon is

$$E_{\max} = \frac{M}{2} \left( \frac{M}{m_1 + m_2} - \frac{m_1 + m_2}{M} \right). \quad (\text{B.5})$$

2. The azimuthal angle  $\phi$  is randomly generated between 0 and  $2\pi$ .
3. The generation of the polar angle  $\theta$  is more complicated. The polar angle is generated by only using the interference term *i.e.* neglecting mass terms. This term is first rewritten

$$\frac{1}{(1 - \beta_1 c)(1 + \beta_2 c)} = \frac{\beta_1 \beta_2}{\beta_1 + \beta_2} \left( \frac{1}{\beta_2 (1 - \beta_1 c)} + \frac{1}{\beta_1 (1 + \beta_2 c)} \right). \quad (\text{B.6})$$

The angle can then be generated according to this distribution by generating the angle according to the distribution  $(1 - \beta_1 c)^{-1}$  with probability

$$P_1 = \frac{\ln \left( \frac{1+\beta_1}{1-\beta_1} \right)}{\ln \left( \frac{1+\beta_1}{1-\beta_1} \right) + \ln \left( \frac{1+\beta_2}{1-\beta_2} \right)} \quad (\text{B.7})$$

and according to the distribution  $(1 + \beta_2 c)^{-1}$  with probability  $P_2 = 1 - P_1$ .

The full distribution can easily be generated using rejection techniques, the rejection weight

$$\mathcal{W} = \frac{\left( -\frac{1-\beta_1^2}{(1-\beta_1 c)^2} + \frac{2(1+\beta_1\beta_2)}{(1-\beta_1 c)(1+\beta_2 c)} - \frac{1-\beta_2^2}{(1+\beta_2 c)^2} \right)}{\frac{2(1+\beta_1\beta_2)}{(1-\beta_1 c)(1+\beta_2 c)}} \leq 1 \quad (\text{B.8})$$

is less than one.

In practice we sometimes choose not to generate the angle according to the full distribution initially *i.e.* we postpone the latter rejection step until the event is generated in full. This is because the inclusion of the mass terms leads to a depletion of radiation in the direction of the charged particles, the “dead-cone” [44]. However this dead-cone can be filled by hard radiation and if the  $\bar{\beta}_1^1$  corrections are included. In this case, if the generation of the angles is done according to the full distribution, the algorithm becomes very inefficient.

In order to calculate the crude distribution we require the average photon multiplicity, which is given by the integral of the dipole function

$$\begin{aligned} & \int \frac{d^3k}{k_0} \tilde{S}(p_1, p_2, k) \\ &= -\frac{\alpha}{\pi} Z_1 Z_2 \ln\left(\frac{E_{max}}{\omega}\right) \left( \left( \frac{1+\beta_1\beta_2}{\beta_1+\beta_2} \right) \ln\left(\frac{(1-\beta_1)(1-\beta_2)}{(1+\beta_1)(1+\beta_2)}\right) - 2 \right) \text{ full distribution,} \\ &= -\frac{\alpha}{\pi} Z_1 Z_2 \left( \frac{1+\beta_1\beta_2}{\beta_1+\beta_2} \right) \ln\left(\frac{E_{max}}{\omega}\right) \ln\left(\frac{(1-\beta_1)(1-\beta_2)}{(1+\beta_1)(1+\beta_2)}\right) \quad \text{neglecting mass terms.} \end{aligned} \quad (\text{B.9})$$

## B.2 Initial-Final Dipoles

Consider the integral of the dipole function in the rest frame of  $p$

$$\int \frac{d^3k}{k_0} \tilde{S}(p, p_1, k) = -\frac{\alpha}{4\pi^2} Z_p Z_1 \int dc d\phi dk_0 k_0 \left( \frac{p}{p \cdot k} - \frac{p_1}{p_1 \cdot k} \right)^2, \quad (\text{B.10})$$

where  $Z_p$  denotes the charge on the decaying particle. As before we choose to define the photon momenta as being with respect to  $p_1$  hence the integral may be rewritten

$$\int \frac{d^3k}{k_0} \tilde{S}(p, p_1, k) = \frac{\alpha}{4\pi^2} Z_p Z_1 \int dc d\phi d \ln k_0 \frac{\beta_1^2 (1 - c^2)}{(1 - \beta_1 c)^2}. \quad (\text{B.11})$$

The photon energy and azimuthal angle are generated in exactly the same way as in appendix (B.1) with the exception that now, to guarantee the possibility of conserving momentum in the decaying particle’s rest frame, the maximum allowable energy of the photons is

$$E_{max} = \frac{M}{2} \left( 1 - \frac{(m_1 + m_2)^2}{M^2} \right). \quad (\text{B.12})$$

The generation of the polar angle  $\theta$  is more straightforward than for the final-final dipole. Omitting the mass terms  $p_1^2$  and  $p^2$  in (B.10) leads to the replacement

$$\frac{\beta_1^2 (1 - c^2)}{(1 - \beta_1 c)^2} \rightarrow \frac{2}{1 - \beta_1 c}, \quad (\text{B.13})$$

which may be generated by the simple mapping

$$c = \frac{1}{\beta_1} \left( 1 - (1 + \beta_1) \left( \frac{1 - \beta_1}{1 + \beta_1} \right)^{\mathcal{R}} \right). \quad (\text{B.14})$$

The full distribution can be recovered by weighting and rejecting the events from this approximate distribution, with weight

$$\mathcal{W} = \frac{\beta_1^2 (1 - c^2)}{2(1 - \beta_1 c)} \leq 1. \quad (\text{B.15})$$

As with the final-final dipole the integral of the dipole function gives the average photon multiplicity for  $\Gamma_{\text{crude}}$ :

$$\begin{aligned} & \int \frac{d^3k}{k_0} \tilde{S}(p, p_1, k) \\ &= \frac{\alpha}{\pi} Z_p Z_1 \ln \left( \frac{E_{\text{max}}}{\omega} \right) \left( \frac{1}{\beta_1} \ln \left( \frac{1 + \beta_1}{1 - \beta_1} \right) - 2 \right) \text{ full distribution} \\ &= \frac{\alpha}{\pi} Z_p Z_1 \ln \left( \frac{E_{\text{max}}}{\omega} \right) \left( \frac{1}{\beta_1} \ln \left( \frac{1 + \beta_1}{1 - \beta_1} \right) \right) \text{ neglecting mass terms.} \end{aligned} \quad (\text{B.16})$$

## References

- [1] P. Richardson, *Spin Correlations in Monte Carlo Simulations*, *JHEP* **11** (2001) 029, [[hep-ph/0110108](#)].
- [2] S. Catani, F. Krauss, R. Kuhn, and B. R. Webber, *QCD Matrix Elements + Parton Showers*, *JHEP* **11** (2001) 063, [[hep-ph/0109231](#)].
- [3] S. Frixione and B. R. Webber, *Matching NLO QCD Computations and Parton Shower Simulations*, *JHEP* **06** (2002) 029, [[hep-ph/0204244](#)].
- [4] S. Gieseke, P. Stephens, and B. Webber, *New Formalism for QCD Parton Showers*, *JHEP* **12** (2003) 045, [[hep-ph/0310083](#)].
- [5] T. Gleisberg *et al.*, *SHERPA 1.α, A Proof-of-Concept Version*, *JHEP* **02** (2004) 056, [[hep-ph/0311263](#)].
- [6] M. Bertini, L. Lonnblad, and T. Sjostrand, *Pythia Version 7-0.0: A Proof-of-Concept Version*, *Comput. Phys. Commun.* **134** (2001) 365–391, [[hep-ph/0006152](#)].
- [7] L. Lonnblad, *Status of the PYTHIA7 Project*, *Nucl. Instrum. Meth.* **A502** (2003) 549–551.

- [8] S. Gieseke, A. Ribon, M. H. Seymour, P. Stephens, and B. Webber, *Herwig++ 1.0: An Event Generator for  $e^+e^-$  Annihilation*, *JHEP* **02** (2004) 005, [[hep-ph/0311208](#)].
- [9] S. Gieseke, *The new Monte Carlo event generator Herwig++*, [hep-ph/0408034](#).
- [10] S. Gieseke *et al.*, *Herwig++ 2.0 $\beta$  Release Note*, [hep-ph/0602069](#).
- [11] D. Grellscheid, K. Hamilton, and P. Richardson, “Simulation of Hadronic Decays in the Herwig++ Event Generator.” In preparation.
- [12] E. Barberio and Z. Was, *PHOTOS: A Universal Monte Carlo for QED Radiative Corrections. Version 2.0*, *Comput. Phys. Commun.* **79** (1994) 291–308.
- [13] E. Barberio, B. van Eijk, and Z. Was, *PHOTOS: A Universal Monte Carlo for QED Radiative Corrections in Decays*, *Comput. Phys. Commun.* **66** (1991) 115–128.
- [14] P. Golonka and Z. Was, *PHOTOS Monte Carlo: A Precision Tool for QED Corrections in Z and W decays*, [hep-ph/0506026](#).
- [15] D. R. Yennie, S. C. Frautschi, and H. Suura, *The Infrared Divergence Phenomena and High-energy Processes*, *Ann. Phys.* **13** (1961) 379–452.
- [16] S. Jadach, *Yennie-Frautschi-Suura Soft Photons in Monte Carlo Event Generators*, . MPI-PAE/PTh 6/87.
- [17] S. Jadach and B. F. L. Ward, *Exponentiation of Soft Photons in the Monte Carlo: The Case of Bonneau and Martin*, *Phys. Rev.* **D38** (1988) 2897.
- [18] S. Jadach and B. F. L. Ward, *YFS2: The Second Order Monte Carlo for Fermion Pair Production at LEP/SLC with the Initial State Radiation of Two Hard and Multiple Soft Photons*, *Comput. Phys. Commun.* **56** (1990) 351–384.
- [19] S. Jadach, B. F. L. Ward, and Z. Was, *Coherent Exclusive Exponentiation for Precision Monte Carlo Calculations*, *Phys. Rev.* **D63** (2001) 113009, [[hep-ph/0006359](#)].
- [20] S. Jadach, B. F. L. Ward, and Z. Was, *The Precision Monte Carlo Event Generator KK for 2-Fermion Final States in  $e^+e^-$  Collisions*, *Comput. Phys. Commun.* **130** (2000) 260–325, [[hep-ph/9912214](#)].
- [21] W. Placzek and S. Jadach, *Multiphoton Radiation in Leptonic W-Boson Decays*, *Eur. Phys. J.* **C29** (2003) 325–339, [[hep-ph/0302065](#)].
- [22] S. Jadach, W. Placzek, M. Skrzypek, B. F. L. Ward, and Z. Was, *The Monte Carlo Program KoralW version 1.51 and The Concurrent Monte Carlo KoralW & YFSWW3 with All Background Graphs and First-Order Corrections to W-Pair Production*, *Comput. Phys. Commun.* **140** (2001) 475–512, [[hep-ph/0104049](#)].

- [23] S. Jadach, W. Placzek, M. Skrzypek, B. F. L. Ward, and Z. Was, *The Monte Carlo Event Generator YFSWW3 version 1.16 for W-Pair Production and Decay at LEP2/LC Energies*, *Comput. Phys. Commun.* **140** (2001) 432–474, [[hep-ph/0103163](#)].
- [24] U. Baur and D. Zeppenfeld, *Finite Width Effects and Gauge Invariance in Radiative W Productions and Decay*, *Phys. Rev. Lett.* **75** (1995) 1002–1005, [[hep-ph/9503344](#)].
- [25] U. Baur, O. Brein, W. Hollik, C. Schappacher, and D. Wackerth, *Electroweak Radiative Corrections to Neutral-Current Drell-Yan Processes at Hadron Colliders*, *Phys. Rev.* **D65** (2002) 033007, [[hep-ph/0108274](#)].
- [26] U. Baur and D. Wackerth, *Electroweak Radiative Corrections to  $p\bar{p} \rightarrow W^\pm \rightarrow l^\pm\nu$  Beyond The Pole Approximation*, *Phys. Rev.* **D70** (2004) 073015, [[hep-ph/0405191](#)].
- [27] C. M. Carloni Calame, G. Montagna, O. Nicrosini, and M. Treccani, *Higher-order QED corrections to W-boson mass determination at hadron colliders*, *Phys. Rev.* **D69** (2004) 037301, [[hep-ph/0303102](#)].
- [28] C. M. Carloni Calame, G. Montagna, O. Nicrosini, and M. Treccani, *Multiple photon corrections to the neutral-current Drell-Yan process*, *JHEP* **05** (2005) 019, [[hep-ph/0502218](#)].
- [29] S. Dittmaier and M. Kramer, *Electroweak radiative corrections to W-boson production at hadron colliders*, *Phys. Rev.* **D65** (2002) 073007, [[hep-ph/0109062](#)].
- [30] D. Wackerth and W. Hollik, *Electroweak Radiative Corrections to Resonant Charged Gauge Boson Production*, *Phys. Rev.* **D55** (1997) 6788–6818, [[hep-ph/9606398](#)].
- [31] E. N. Argyres *et al.*, *Stable Calculations for Unstable Particles: Restoring Gauge Invariance*, *Phys. Lett.* **B358** (1995) 339–346, [[hep-ph/9507216](#)].
- [32] W. Beenakker *et al.*, *The Fermion-Loop Scheme for Finite-Width Effects in  $e^+e^-$  Annihilation into Four Fermions*, *Nucl. Phys.* **B500** (1997) 255–298, [[hep-ph/9612260](#)].
- [33] B. F. L. Ward, *Renormalization-group-improved Yennie-Frautschi-Suura theory*, *Phys. Rev.* **D36** (1987) 939.
- [34] S. Jadach, W. Placzek, M. Skrzypek, and B. F. L. Ward, *Gauge-invariant YFS exponentiation of (un)stable  $W^+W^-$  production at and Beyond LEP2 energies*, *Phys. Rev.* **D54** (1996) 5434–5442, [[hep-ph/9606429](#)].
- [35] S. Jadach, “Monte Carlo Methods for High Energy Physics.” Lectures at the Torino School of Physics, 2001. Available from <http://jadach.home.cern.ch/jadach/>.
- [36] R. Kleiss and W. J. Stirling, *Massive Multiplicities and Monte Carlo*, *Nucl. Phys.* **B385** (1992) 413–432.

- [37] S. Catani, S. Dittmaier, and Z. Trocsanyi, *One-Loop Singular Behaviour of QCD and SUSY QCD Amplitudes with Massive Partons*, *Phys. Lett.* **B500** (2001) 149–160, [hep-ph/0011222].
- [38] S. Catani, S. Dittmaier, M. H. Seymour, and Z. Trocsanyi, *The Dipole Formalism for Next-to-Leading Order QCD Calculations with Massive Partons*, *Nucl. Phys.* **B627** (2002) 189–265, [hep-ph/0201036].
- [39] F. Bloch and A. Nordsieck, *Note on the Radiation Field of the Electron*, *Phys. Rev.* **52** (1937) 54–59.
- [40] T. Kinoshita, *Mass Singularities of Feynman Amplitudes*, *J. Math. Phys.* **3** (1962) 650–677.
- [41] T. D. Lee and M. Nauenberg, *Degenerate Systems and Mass Singularities*, *Phys. Rev.* **133** (1964) B1549–B1562.
- [42] W. J. Marciano and A. Sirlin, *Deviations from Electron-Muon Universality in the Leptonic Decays of the Intermediate Bosons*, *Phys. Rev.* **D8** (1973) 3612–3615.
- [43] C. M. Carloni Calame, S. Jadach, G. Montagna, O. Nicrosini, and W. Placzek, *Comparisons of the Monte Carlo programs HORACE and WINHAC for Single W-boson Production at Hadron Colliders*, *Acta Phys. Polon.* **B35** (2004) 1643–1674, [hep-ph/0402235].
- [44] G. Marchesini and B. R. Webber, *Simulation of QCD Coherence in Heavy Quark Production and Decay*, *Nucl. Phys.* **B330** (1990) 261.